Construction of a semilocal exchange density functional from a three-dimensional electron gas collapsing to two dimensions

C. M. Horowitz[*]

*Instituto de Investigaciones Fisicoquímicas Teóricas y Aplicadas, (INIFTA), UNLP, CCT La Plata-CONICET,
Sucursal 4, Casilla de Correo 16, (1900) La Plata. Argentina*

C. R. Proetto[†]

*Centro Atómico Bariloche and Instituto Balseiro (Universidad Nacional de Cuyo), 8400 S. C. de Bariloche, Río Negro, Argentina
and Instituto de Nanociencia y Nanotecnología (INN), CONICET-CNEA, Sede Bariloche Av. Bustillo 9500 (8400)
S. C. de Bariloche, Río Negro, Argentina*

J. M. Pitarke[‡]

*CIC nanoGUNE BRTA, Tolosa Hiribidea 76, E-20018 Donostia, Basque Country, Spain
and Fisika Saila, Centro Física Materiales CSIC-UPV/EHU, and DIPC, 644 Posta Kutxatila, E-48080 Bilbo, Basque Country, Spain*

In a recent paper [Horowitz *et al.*, Phys. Rev. B **107**, 195120 (2023)], an alternative route has been proposed to construct the so-called exchange-correlation (xc) enhancement factor F_{xc} of density-functional theory, defined as the enhancement of a realistic xc energy density over its local exchange-only counterpart. This new route, based on the *ab initio* calculation of the exact exchange energy density of a family of electron-density profiles, was implemented on the basis of jellium-slab exact-exchange self-consistent calculations. Here, we follow this route to construct a meta-generalized-gradient approximation (MGGA) for exchange from a nonuniform one-dimensional coordinate scaling, which we implement on the basis of a number of calculations performed for model densities of electrons confined by infinite-barrier walls, as the electron system is shrunk from three to two dimensions. Our MGGA yields exchange energies that approach in the two-dimensional (2D) limit the exact exchange energy of a 2D electron gas, by appealing to a scaling of the MGGA exchange enhancement factor.

I. INTRODUCTION

Density-functional theory (DFT) is well known to be widely used nowadays for the description of many-electron systems by introducing, as the basic variable, the ground-state electron density $n(\mathbf{r})$ [1,2]. This formalism, however, relies on the knowledge of a generally unknown quantity, which is the so-called exchange-correlation (xc) energy functional $E_{xc}[n]$ that needs to be approximated [3]. A hierarchy of local, semilocal, and fully nonlocal approximations can be found in Ref. [4]. Here, we focus on the development of a semilocal approximation: the so-called meta-generalized-gradient approximation (MGGA) [5–7], which relies on the knowledge of the dimensionless reduced density gradient,

$$s(\mathbf{r}) = \frac{|\nabla n(\mathbf{r})|}{2(3\pi^2)^{1/3} n(\mathbf{r})^{4/3}} \tag{1}$$

and the parameter

$$\alpha(\mathbf{r}) = \frac{t(\mathbf{r}) - t^{\mathrm{W}}(\mathbf{r})}{t^{\mathrm{unif}}(\mathbf{r})}, \tag{2}$$

where t is the kinetic-energy density [8,9], $t^{\mathrm{W}} = |\nabla n|^2/8n$ represents its von Weizsäcker counterpart [8,9], and $t^{\mathrm{unif}} = (3/10)(3\pi^2)^{2/3} n^{5/3}$ is the kinetic-energy density of a three-dimensional (3D) spin-compensated uniform electron gas. Since t^{W} is known to be a lower bound of t [10], $\alpha \geqslant 0$. The reduced density gradient $s(\mathbf{r})$ represents a measure of the variation of the density at the scale of the local Fermi wave length λ_F, and the parameter $\alpha(\mathbf{r})$ is sometimes referred to as a dimensionless deviation of an arbitrary many-electron system from single-orbital shape.

Available MGGAs are either (i) semiempirical functionals, built to best reproduce existing data of real systems of interest (see, e.g., Ref. [5]); or (ii) nonempirical functionals, constructed to satisfy exact constraints (see, e.g., Refs. [6,7]). Here, we follow an alternative route [11], based on the *ab initio* calculation of the exact exchange energy of a family of electron-density profiles, which we now take to be model densities of electrons confined in one direction by infinite-barrier walls, as the electron system is shrunk from three to two dimensions by means of a nonuniform one-dimensional coordinate scaling. This allows us to propose a new MGGA that describes very well the dimensional crossover of the exact exchange functional and should be particularly suited for the description of two-dimensional (2D) systems [12,13], layered van der Waals materials [14], and surfaces of transition metals [15].

[*]horowitz@inifta.unlp.edu.ar
[†]proetto@cab.cnea.gov.ar
[‡]jm.pitarke@nanogune.eu

The present work is organized as follows: The nonuniform one-dimensional coordinate scaling and the infinite barrier model are introduced in Secs. II and III. We then describe, in Sec. IV, our so-called generalized and MGGA exchange enhancement factors, which lead, in Sec. V, to a parametrized MGGA that we test for the exchange energy of a many-electron system as it shrinks from three to two dimensions. We find that our MGGA yields exchange energies that approach, in the 2D limit, the exact exchange energy of a 2D electron gas.

II. NONUNIFORM ONE-DIMENSIONAL COORDINATE SCALING

Coordinate scaling represents a valuable tool in the development of xc-energy functionals, as it leads to exact constraints that exact functionals should meet. Here, we take a many-electron slab with translational invariance in a plane normal to the z axis, and we consider a nonuniform one-dimensional coordinate scaling of the 3D density of the form

$$n(z) \rightarrow n_\lambda(z) := \lambda\, n(\lambda z), \qquad (3)$$

with $0 < \lambda < \infty$. Under this scaling, the bidimensional density $N/A := \int dz\, n(z)$ remains the same and the true 2D limit is reached as $\lambda \rightarrow \infty$.

For a many-electron system that is finite along the z axis and in a quasi-2D regime with only one occupied slab discrete energy level (SDL = 1), the exact exchange energy functional per electron is found to be given by the following expression [16–18]:

$$\frac{E_x[n]}{N} = -\frac{4\pi^2 e^2}{\left(k_F^{2D}\right)^4} \int_{-\infty}^{\infty} dz \int_{-\infty}^{\infty} dz'\, F(|z-z'|)\, n(z)\, n(z'), \qquad (4)$$

where N represents the total number of electrons, $k_F^{2D} = 2\pi/\lambda_F^{2D}$ (λ_F^{2D} being the 2D Fermi wave length), and

$$F(y) = \frac{1}{2|y|}\left[1 - \frac{I_1\left(2k_F^{2D}|y|\right)}{k_F^{2D}|y|} + \frac{L_1\left(2k_F^{2D}|y|\right)}{k_F^{2D}|y|}\right], \qquad (5)$$

I_1 and L_1 being, respectively, modified Bessel and Struve functions of the first kind. The 2D Fermi wave length is $\lambda_F^{2D} = \sqrt{2}\pi r_s^{2D} a_0$, with r_s^{2D} being the dimensionless 2D Seitz radius, i.e., the radius of the section (in the x-y plane) that encloses on average one electron, i.e., $\pi(a_0 r_s^{2D})^2 = A/N$; here, a_0 denotes the atomic Bohr radius and A represents a normalization area in the x-y plane. Using Eq. (3) and expanding in the limit $\lambda \gg 1$ (2D limit), we find

$$\frac{E_x[n_\lambda]}{N} = -\frac{4e^2 k_F^{2D}}{3\pi} + \frac{\pi^2 e^2}{\left(k_F^{2D}\right)^2 \lambda} \int_{-\infty}^{\infty} dz \int_{-\infty}^{\infty} dz'\, |z-z'|$$
$$\times\, n(z)\, n(z')$$
$$- \frac{32\pi e^2}{45 k_F^{2D} \lambda^2} \int_{-\infty}^{\infty} dz \int_{-\infty}^{\infty} dz'\, |z-z'|^2\, n(z)\, n(z')$$
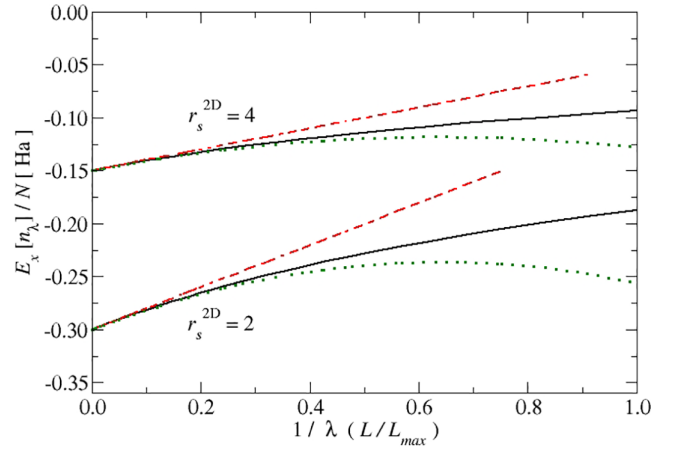$$+ O[\lambda^{-3}]. \qquad (6)$$

FIG. 1. $E_x[n_\lambda]/N$, as a function of $L/L_{\max} = 1/\lambda$, for the IBM electron density of Eq. (7) and for two values of r_s^{2D}: 2 and 4. The solid lines represent the exact $E_x[n_\lambda]/N$, as obtained from Eq. (4). Dashed (red) and dotted (green) lines represent $E_x[n_\lambda]/N$, as obtained from Eq. (6) up to first order in $1/\lambda$ and up to second order in $1/\lambda$, respectively.

In obtaining the first term of Eq. (6), we have taken into account that $\int_{-\infty}^{\infty} dz\, n(z) = (k_F^{2D})^2/(2\pi)$. This term, which represents the strict 2D limit, coincides, as expected, with the well-known expression for the exchange energy per particle of a uniform 2D electron gas [19]. The second term, which scales as λ^{-1}, cancels out exactly half of the Hartree contribution to the slab total energy for a spin-compensated system as we are considering here. It is easy to see that for a fully spin-polarized many-electron slab, the cancellation is complete.

Equations (4)–(6) describe the exchange energy per particle of an arbitrary many-electron system in the quasi-2D regime. For the practical evaluation of this quantity with the electron density $n_\lambda(z)$ dictated by Eq. (3), we model the slab as a quantum well of thickness L in the z direction. In the infinite barrier model (IBM) [20], which is well suited for the description of the nonuniform one-dimensional coordinate scaling of Eq. (3), the Kohn-Sham (KS) effective one-electron potential is replaced by zero inside infinitely high potential walls at $z = 0$ and $z = L$. The quasi-2D regime, where only the lowest energy level is occupied in the z direction, occurs when $L < L_{\max}$, with $L_{\max} = \sqrt{3}\,\lambda_F^{2D}/2$ [21]. In this regime, the IBM electron density at $0 \leqslant z \leqslant L$ is simply

$$n(z) = \frac{4\pi}{L\left(\lambda_F^{2D}\right)^2}\sin^2\left(\frac{\pi z}{L}\right), \qquad (7)$$

and vanishes for $z \leqslant 0$ and $z \geqslant L$. By replacing in Eq. (7) the quantum-well thickness L by L/λ, the scaled electron density $n_\lambda(z)$ of Eq. (3) is obtained.

We display in Fig. 1 the exchange energy per particle $E_x[n_\lambda]/N$ of Eq. (4), as a function of $L/L_{\max} = 1/\lambda$, together with the expansion of Eq. (6) up to first order (dashed lines) and second order (dotted lines). The bidimensional density N/A is kept constant in this model, so the curves in this figure are all fully determined by the particular value of r_s^{2D} alone. The exact values of the exchange energy per particle as $\lambda \rightarrow \infty$ are $E_x[n_\lambda]/N = -0.150$ Ha and -0.300 Ha, for $r_s^{2D} = 4$ and $r_s^{2D} = 2$, respectively.

We note that under the scaling of Eq. (3), the MGGA parameters $s(z)$ and $\alpha(z)$ scale with λ as follows:

$$s[n](z) = \frac{|dn(z)/dz|}{2(3\pi^2)^{1/3}n(z)^{4/3}} \rightarrow s[n_\lambda](z) = \lambda^{2/3}s[n](\lambda z) \quad (8)$$

and

$$\alpha[n](z) = \frac{5}{3(3\pi^2)^{2/3}(r_s^{2D})^2}\frac{1}{n(z)^{2/3}} \rightarrow$$

$$\alpha[n_\lambda](z) = \lambda^{-2/3}\alpha[n](\lambda z). \quad (9)$$

As the electron system collapses from three to two dimensions ($\lambda \rightarrow \infty$), $s[n_\lambda](z)$ diverges, while $\alpha[n_\lambda](z)$ becomes arbitrarily small [22]; the product of these two quantities stays, however, finite. It should be noted that the simple expression for $\alpha[n](z)$ in Eq. (9) is only valid for SDL = 1.

III. INFINITE BARRIER MODEL BEYOND THE QUASI-2D REGIME

Still in the IBM but beyond the quasi-2D regime, the electron density at $0 \leqslant z \leqslant L$ normalized by the density of a neutralizing positive background n_+ is found to be given by the following expression [20]:

$$\frac{n(z)}{n_+} = \frac{3}{2x}\sum_{l=1}^{l_M}\left(1 - \frac{l^2}{4x^2}\right)\sin^2\left(\frac{\pi l z}{L}\right), \quad (10)$$

where $x = L/\lambda_F$, l_M denotes the highest occupied energy level, and λ_F is the 3D Fermi wave length $\lambda_F = (32\pi^2/9)^{1/3}r_s a_0$, and r_s being the dimensionless 3D Seitz radius. Besides, n_+ represents the density of a neutralizing jellium background at $-a/2 < z < a/2$, the quantity a being dictated by a global neutrality condition [20]. For $l_M = 1$, Eq. (7) is recovered. The densities $n(z)$ and n_+ both depend on r_s. However, the normalized electron density $n(z)/n_+$ of Eq. (10), as well as the parameters $s(z)$ and $\alpha(z)$, are easily found to be "universal," i.e., independent of r_s and r_s^{2D}, as long as the coordinate z and the quantum-well thickness L are both expressed in units of λ_F and λ_F^{2D}, respectively (see the Appendix).

The normalized electron density of Eq. (10) is displayed in Fig. 2, together with the corresponding parameters $s(z)$ and $\alpha(z)$ for various values of the quantum-well thickness: (i) $L = 0.8\,\lambda_F$, with one single energy level occupied ($l_M = 1$); (ii) $L = 1.6\,\lambda_F$ ($l_M = 3$); and (iii) $L = 2.6\,\lambda_F$ ($l_M = 5$). All curves are universal, i.e., the same for all values of r_s. We note that the normalized density (i) vanishes at the infinite barrier at $z = L$ and (ii) approaches—well inside the larger slabs—its bulk value $n(z)/n_+ = 1$. As for the parameters $s[n](z)$ and $\alpha[n](z)$, they both diverge at the infinite barrier. Well inside the slab, the parameter $s[n](z)$ vanishes every time the density is minimum or maximum, while the parameter $\alpha[n](z)$ oscillates and approaches its unit bulk value as L increases.

It should be noted that in our quantum-well "training set" of densities to be used in the next section, densities with small values of $\alpha(z)$ are not common, unless one drives the quantum well toward the extreme quantum limit, in which case and according to Eq. (9) arbitrarily small values of $\alpha(z)$ become accessible. This is visible in Fig. 2(c), where the smallest $\alpha(z)$ occurs, near the quantum-well center, for the narrowest slab.
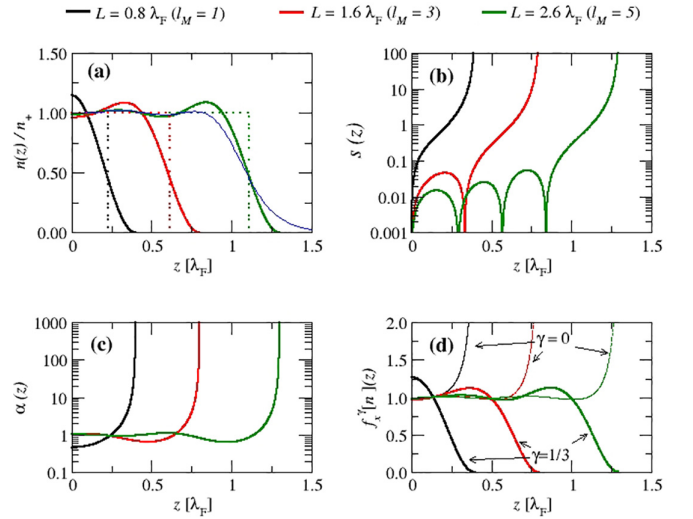

FIG. 2. Normalized electron density $n(z)/n_+$, $s(z)$, $\alpha(z)$, and the generalized enhancement factor $f_x^\gamma[n](z)$ of Eq. (11), versus z/λ_F, for three different quantum-well widths: $L/\lambda_F = 0.8$, with $l_M = 1$ (black curves); $L/\lambda_F = 1.6$, with $l_M = 3$ (red curves); and $L/\lambda_F = 2.6$, with $l_M = 5$ (green curves). Thick and thin curves in panel (d) correspond to $\gamma = 1/3$ and $\gamma = 0$, respectively. For comparison, in the case of the largest slab ($L/\lambda_F = 2.6$) the corresponding self-consistent (with no external potential) normalized electron density $n(z)/n_+$ is represented (for $r_s = 2$) by a blue curve in panel (a). The neutralizing jellium background at $-a/2 < z < a/2$ is represented by dotted horizontal and vertical lines. In all cases, $z = 0$ is at the middle of the quantum well, resulting in a right-wall location at $z = L/2$. All IBM curves are universal, i.e., the same for all values of r_s.

IV. GENERALIZED AND MGGA EXCHANGE ENHANCEMENT FACTORS

Now we define a generalized exchange enhancement factor as follows [11]:

$$f_x^\gamma[n](z) := \frac{\varepsilon_x^\gamma[n](z)}{\varepsilon_x^{\text{unif}}(n(z))}, \quad (11)$$

where $\varepsilon_x^{\text{unif}}(n) = -(3e^2/4\pi)(3\pi^2 n)^{1/3}$ is the exchange energy per particle of a spin-compensated 3D uniform system of electron density n, and $\varepsilon_x^\lambda[n](z)$ represents a γ-transformed exact exchange energy per particle:

$$\varepsilon_x^\gamma[n](z) = \frac{-2e^2}{n(z)}\sum_{l,l'}^{occ.}\int_{-\infty}^{\infty}dz'\,\gamma_{ll'}[(1+\gamma)z - \gamma z']$$

$$\times g_{ll'}(|z - z'|)\gamma_{l'l}[\gamma z + (1-\gamma)z'], \quad (12)$$

which integrates to the total exchange energy:

$$E_x[n] = A\int_{-\infty}^{\infty}dz\,n(z)\,\varepsilon_x^\gamma[n](z)$$

$$= A\int_{-\infty}^{\infty}dz\,n(z)\,\varepsilon_x^{\text{unif}}(n(z))\,f_x^\gamma[n](z) \quad (13)$$

for all values of γ ($0 \leqslant \gamma \leqslant 1$). Here, $\gamma_{ll'}(z) = \phi_l^*(z)\phi_{l'}(z)$, with $\phi_l(z)$ being occupied single-particle orbitals, and [23]

$$g_{ll'}(u) = \frac{k_F^l k_F^{l'}}{4\pi} \int_0^\infty \frac{d\rho}{\rho} \frac{J_1(\rho k_F^l)J_1(\rho k_F^{l'})}{\sqrt{\rho^2 + u^2}}, \quad (14)$$

with $J_1(x)$ being the cylindrical Bessel function of the first order and $k_F^l = \sqrt{2m(\mu - \varepsilon_l)}/\hbar$. Here, ε_l are single-particle energies and μ represents the chemical potential, which is determined from the global neutrality condition. In the IBM, the normalized single-particle orbitals and energies are

$$\phi_l(z) = \sqrt{\frac{2}{L}} \sin\left(\frac{\pi l z}{L}\right)\theta(z)\theta(L-z) \quad (15)$$

and

$$\varepsilon_l = \frac{\hbar^2}{2m}\left(\frac{l\pi}{L}\right)^2, \quad (16)$$

with $l = 1, 2, ...,$ and the electron density is given by Eq. (10). Figure 2(d) displays the generalized exchange enhancement factor $f_x^\gamma[n](z)$ for $\gamma = 0$ and for $\gamma = 1/3$, and for quantum wells of increasing size. For $\gamma = 0$, the so-called "conventional" choice, the generalized exchange enhancement factor diverges when z approaches the infinite barrier and cannot, therefore, be expressed as a bounded enhancement factor that fulfills the local Lieb-Oxford (LO) lower bound on the exchange energy [24]. For $0 < \gamma < 1$, however, $f_x^\gamma[n](z)$ is always bounded [25]. Here, we choose $\gamma = 1/3$, as in our previous work [11].

In the MGGA [26], one writes

$$E_x^{\text{MGGA}}[n] = A \int_{-\infty}^\infty dz\, n(z)\, \varepsilon_x^{\text{unif}}(n(z))\, F_x(s(z), \alpha(z)), \quad (17)$$

where $F_x(s, \alpha)$ is the so-called MGGA exchange enhancement factor, which we build by simply comparing Eqs. (13) and (17). With this purpose in mind, we first calculate $s(z)$, $\alpha(z)$, and $f_x^\gamma[n](z)$ in the IBM, for many different values of the normalized quantum-well thickness L/λ_F and within each L/λ_F for a large number of normalized z/λ_F coordinates. We have considered on the order of 1000 z coordinates and about 10 000 different values of L/λ_F, from sufficiently large quantum wells to very narrow wells in the 2D limit ($L \to 0$). It is not difficult to see from Eq. (11) that in the IBM the generalized exchange enhancement factor $f_x^\gamma[n](z)$ is universal, i.e., independent of the 3D Seitz radii r_s and r_s^{2D}, as in the case of the normalized electron density $n(z)/n_+$ and the parameters $s(z)$ and $\alpha(z)$. An explicit proof of this universality is given in the Appendix. Proceeding in this way, we obtain numerically the mapping $f_x^\gamma[n](z) \to f_x^\gamma[n](s, \alpha)$.

Depending on the electron-density profile $n(z)$, various values of $f_x^\gamma[n](s, \alpha)$ correspond to the very same values of s and α, as expected. This fact is visible in Fig. 3, where we have plotted, as a function of the reduced density gradient s, the exchange enhancement factors $f_x^\gamma[n](s, \alpha)$ that we have obtained for fixed values of the parameter α (colored dots). For the electron densities under study, the exchange enhancement factor $f_x^\gamma[n](s, \alpha)$ is mostly uniquely defined as a function of s and α, but a few narrow bands are visible for the largest values of α under consideration, generally coming from large values of the normalized quantum-well thickness
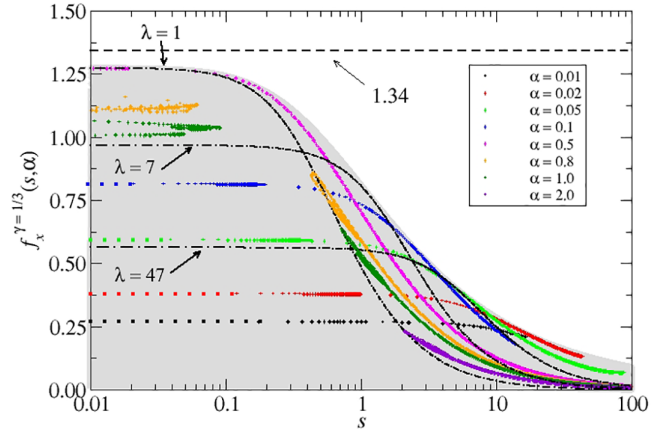

FIG. 3. Colored dots represent the exchange enhancement factor $f_x^{\gamma=1/3}(s, \alpha)$, as obtained from Eq. (11) for those z coordinates corresponding to given values of s and α and a large variety of quantum-well thicknesses L, both below and above L_{max}. The gray area covers the exchange enhancement factors $f_x^{\gamma=1/3}(s, \alpha)$ obtained for all possible values of the parameter α. Dashed dotted lines represent the exchange enhancement factor we obtain, as a function of s, each for a specific quantum-well thickness $L/L_{\text{max}} = 1/\lambda$, going from $L = L_{\text{max}}$ ($\lambda = 1$) to thinner quantum wells with $\lambda = 7$ and $\lambda = 47$. The dashed horizontal line represents the 3D local Lieb-Oxford (LO) bound $B = 1.3423$.

L/λ_F allowing for Friedel oscillations. As the quantum well is made to collapse from three to two dimensions, various values of the parameter α occur, with α getting smaller as $L \to 0$. The gray area covers all possible values of $f_x^\gamma[n](s, \alpha)$ that we have found numerically through the generation of thousands of quantum-well densities. We note that the results exhibited in Fig. 3 do not depend on the electron-density parameters r_s and r_s^{2D}, since the IBM exchange enhancement factor is "universal," as discussed above. This is not so for the self-consistent electron-density profiles discussed in Ref. [11].

The dashed horizontal line in Fig. 3 represents the 3D local Lieb-Oxford (LO) bound $B = 1.3423$ (see, e.g., Refs. [27,28]), which stays above our exchange enhancement factor $f_x^\gamma(s, \alpha)$ for all electron densities under study, as long as $0 < \gamma < 1$. This LO bound has been discussed and extended to lower dimensional cases in Ref. [29].

V. PARAMETRIZED MGGA EXCHANGE ENHANCEMENT FACTOR

In Fig. 4, we have plotted, as a function of the parameter α and on a log-log scale, all generalized exchange enhancement factors $f_x^{\gamma=1/3}[n](s, \alpha)$ that we have obtained for various values of the reduced density gradient from $s \sim 0.01$ to $s \sim 40$. This figure clearly shows that $f_x^{\gamma=1/3}[n](s, \alpha)$ increases, for all density gradients, as $\alpha^{1/2}$ for small values of α, while it decreases, also for all density gradients, as $\alpha^{-1/2}$ for larger values of α. On the other hand, the results of Fig. 3 are plotted again in Fig. 5, as a function of the reduced density gradient s and for various values of the parameter α, but now on a log-log scale, showing that $f_x^{\gamma=1/3}[n](s, \alpha)$ remains essentially constant for all values of α when the reduced density gradient s
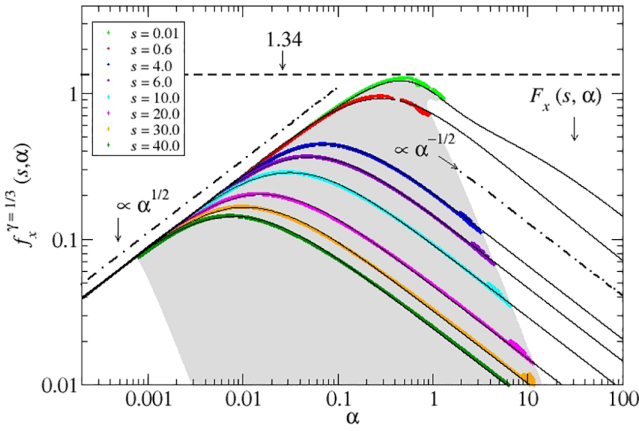
FIG. 4. As in Fig. 3, colored dots represent the exchange enhancement factor $f_x^{\gamma=1/3}(s, \alpha)$, as obtained from Eq. (11) for those z coordinates corresponding to given values of α and s and a large variety of quantum-well thicknesses L, but now as a function of α for various values of s and in a log-log scale. The gray area covers the exchange enhancement factors $f_x^{\gamma=1/3}(s, \alpha)$ obtained for all possible values of the reduced density gradient s. Black solid lines represent our proposed MGGA exchange enhancement factor $F_x(s, \alpha)$ of Eq. (19). For comparison, the dash dotted lines represent $\alpha^{1/2}$ and $\alpha^{-1/2}$ asymptotics for values of the parameter α that are small and large, respectively. The dashed horizontal line represents the 3D local Lieb-Oxford (LO) bound $B = 1.3423$.

is small, while it decreases, again for all values of α, as s^{-1} when the reduced density gradient s is large.

The behavior $f_x^{\gamma=1/3}[n](s, \alpha \to 0) \sim \alpha^{1/2}$ that is clearly visible in Fig. 4 can be derived by first introducing the nonuniform one-dimensional coordinate scaling of Eq. (3) into Eq. (17):

$$E_x^{\mathrm{MGGA}}[n_\lambda] = \lambda^{1/3} A$$

$$\int_{-\infty}^{\infty} dz\, n(z)\, \varepsilon_x^{\mathrm{unif}}(n(z))\, F_x(\lambda^{2/3} s(z), \alpha(z)/\lambda^{2/3}),$$
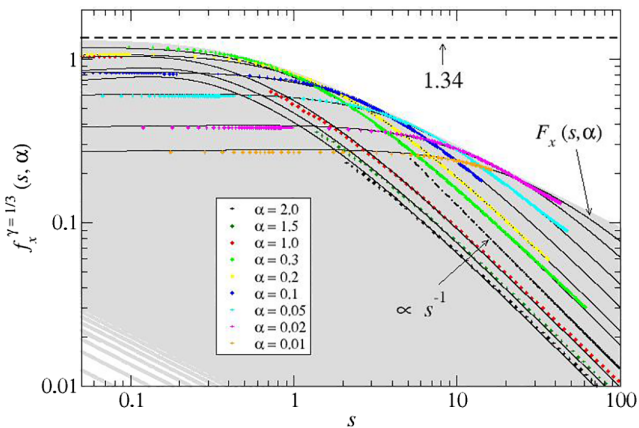
$$(18)$$

FIG. 5. As in Fig. 4, but now as a function of s for various values of α. Here, the gray area covers the exchange enhancement factors $f_x^{\gamma=1/3}(s, \alpha)$ obtained for all possible values of the parameter α, black solid lines represent our proposed MGGA exchange enhancement factor $F_x(s, \alpha)$ of Eq. (19), and the dash dotted line represents the asymptotics dictated by s^{-1}.

and then noticing that for $E_x^{\mathrm{MGGA}}[n_\lambda]$ to stay finite as $\lambda \to \infty$ (collapse to two dimensions) the MGGA exchange enhancement factor $F_x(s, \alpha)$ needs to behave as $F_x(s, \alpha \to 0) \sim \lambda^{-1/3}$, since for $\lambda \gg 1$, $\lambda^{2/3} s \gg 1$ and $\alpha/\lambda^{2/3} \ll 1$. One can then easily conclude from Eq. (9) that $F_x(s, \alpha \to 0) \sim \alpha^{1/2}$.

At the level of the GGA, it can be easily seen from Eq. (8) that for the exchange energy to stay finite as $\lambda \to \infty$ the exchange enhancement factor $F_x(s)$ needs to behave as $F_x(s \to \infty) \sim s^{-1/2}$, as discussed before [7,15,24,30]. Indeed, this was the reason behind the choice $\gamma = 1/3$ in our previous work, as discussed in the Appendix of Ref. [11]. At the level of the MGGA, however, the finite 2D limit is obtained by simply taking $F_x(s, \alpha \to 0) \sim \alpha^{1/2}$ [31], so the large-s limit can be reserved for the satisfaction of other exact constraints; work along this direction is now in progress. The limiting behavior $F_x(s, \alpha \to 0) \sim \alpha^{1/2}$, which is obtained from the nonuniform one-dimensional coordinate scaling of Eq. (3), is not restricted to the IBM electron densities considered above, so it would also apply, in particular, to the self-consistent surface electron densities used, e.g., in Refs. [16–18].

By gathering all the information provided by Figs. 4 and 5, we propose here the following parametrized MGGA exchange enhancement factor:

$$F_x(s, \alpha)$$
$$= \frac{2.7\,\alpha^{1/2}}{1 + 2.7\alpha(0.8788 + s) - A(s)\,\alpha^{B(s)} + 0.924\,\ln(1 + \alpha^3)e^{-10s}},$$
$$(19)$$

where $A(s) = 2.5/(5 + s)^{0.4}$ and $B(s) = 0.96 \times e^{-0.5s^{0.3}}$. This parametrization allows us to identify the following features: (i) $F_x(s, \alpha \to 0) \sim 2.7\,\alpha^{1/2}$; (ii) $F_x(s, \alpha \to \infty) \sim \alpha^{-1/2}/(0.8788 + s)$; (iii) $F_x(s \to 0, \alpha \to 1) \to 1$, fulfilling the bulk limit constraint; and (iv) $F_x(s \to \infty, \alpha) \sim s^{-1}$. Figures 4 and 5 show an excellent agreement between the exchange enhancement factor $f_x^{\gamma=1/3}[n](s, \alpha)$ (colored dots) and our parametrized MGGA of Eq. (19) (solid lines) for all IBM electron densities under study.

With the aim of testing the accuracy of our meta-GGA parametrization, we have evaluated the MGGA exchange energy of Eq. (17) by using Eq. (19) and by also using, for comparison, other existing GGA and MGGA parametrizations: GGA-PBE [32], GGA-Q2D [15], GGA-HPP [11], MGGA-MS [33,34], and MGGA-SCAN [7]. Figure 6 clearly shows that our MGGA [Eq. (19)] yields exchange energies that are in excellent agreement with the exact result for all quantum-well widths, from the strict 2D limit ($L \to 0$) to the quasi-2D regime ($0 < L < L_{\max}$), and also for $L \geqslant L_{\max}$ (see the inset). In particular, our MGGA approaches very accurately, in the 2D limit, the exact exchange energy of a 2D electron gas ($E_x^{2D}/N = -8/(3\sqrt{2\pi} r_s^{2D})(e^2/a_0) = -0.150$ Ha for $r_s^{2D} = 4$), within an error bar of 1%. Most existing MGGAs diverge in the 2D limit, with the exception of the SCAN MGGA [7], which was constructed to fulfill the limiting behavior $F_x(s \to \infty, \alpha) \sim s^{-1/2}$. This constraint guarantees that the exchange energy be finite in the 2D limit, but it leads to a 2D exchange energy per particle that is too negative by an order of magnitude for $r_s^{2D} = 4$, while our constraint $F_x(s, \alpha \to 0) \sim \alpha^{1/2}$ describes the 3D to 2D collapse very accurately. GGAs with the correct limiting behavior $F_x(s \to \infty) \sim s^{-1/2}$, like GGA-Q2D [15] and GGA-

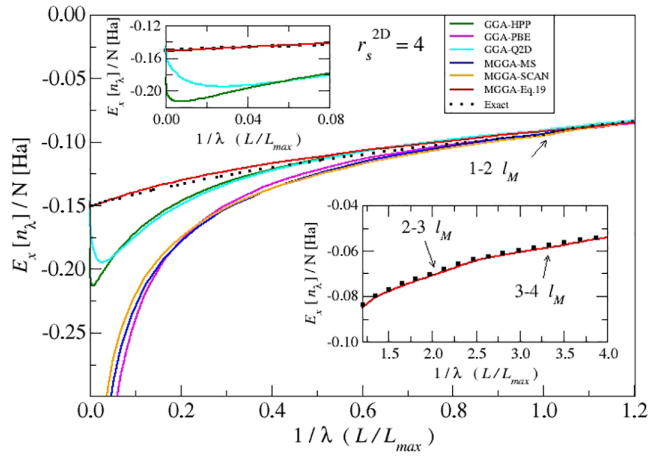FIG. 6. $E_x[n_\lambda]/N$, as function of $L/L_{max} = 1/\lambda$ for the IBM electron density of Eq. (10) with $r_s^{2D} = 4$. The black dotted line represents the exact $E_x[n_\lambda]/N$ of Eq. (13). The red solid line represents the MGGA exchange energy per particle that we have obtained from Eq. (17) by using the exchange enhancement factor of Eq. (19) (this work). The other solid lines represent, for comparison, GGA and MGGA exchange energies per particle obtained by using the the following parametrizations: GGA-PBE [32] (purple), GGA-Q2D [15] (cyan), GGA-HPP [11] (green), MGGA-MS [33,34] (blue), and MGGA-SCAN [7] (orange). The inset at the top shows a zoom of the region near the 2D limit. The inset at the bottom shows a continuation of the dotted line (exact) and solid red line (this work) for larger values of the quantum-well width L. A close inspection of the main figure and the bottom inset shows that the exchange energy exhibits little kinks, with the location of the kinks denoted by arrows. These kinks are the result of a new subband (for the z motion) becoming occupied every time the quantum-well width L increases by a multiple of $\lambda_F/2$.

HPP [11], yield rather accurate values for the 2D exchange energy, but they are still too negative in the quasi-2D regime, as the electron gas collapses from three to two dimensions.

VI. CONCLUSIONS

In summary, we have constructed, from first principles, a MGGA for exchange, by using a non-uniform one-dimensional coordinate scaling that we have implemented on the basis of IBM electron densities as the quantum well shrinks from three to two dimensions. We have found that, at least for our trial set of IBM electron densities, the MGGA exchange enhancement factor $F_x(s, \alpha)$ behaves as (i) $\sim \alpha^{1/2}$ for small values of α, (ii) $\sim \alpha^{-1/2}$ for large values of α, and (iii) $\sim s^{-1}$ for large values of the reduced density gradient s. We have proposed a simple parametrized form of the MGGA enhancement factor $F_x(s, \alpha)$ [Eq. (19)], which has been found to yield exchange energies that are very accurate in the whole range of quantum-well widths and approach in the 2D limit the true finite exchange energy of a 2D electron gas.

A crucial aspect of our parametrization, suggested by both our numerical calculations and analytical scaling arguments, is the fulfillment of the limit $F_x(s, \alpha \to 0) \sim \alpha^{1/2}$. This scaling provides a natural and accurate collapse of the exchange energy per particle toward its finite strict 2D limit, as compared to the scaling $F_x(s \gg 1, \alpha) \sim s^{-1/2}$ employed in

existing MGGA parametrizations for the satisfaction of the same constraint, which leads to a 2D exchange energy per particle that is finite but too negative. We suggest that a $\alpha^{1/2}$ limiting behavior should be generally enforced at small α, while keeping the large-s limit for the satisfaction of other exact constraints, as for example the correct asymptotic behavior of the exchange potential.

As our MGGA describes particularly well the dimensional crossover of the exact exchange functional, it should be well suited for the description of 2D systems, layered van der Waals materials, and transition-metal surfaces.

APPENDIX

In this Appendix, we demonstrate that, in the IBM, the generalized exchange enhancement factor of Eq. (11) is universal, i.e., independent of r_s (r_s^{2D}), as long as the coordinate z and the quantum-well thickness L are both expressed in units of λ_F (λ_F^{2D}).

We start by deriving the scaling of the IBM eigenfunctions of Eq. (15) with respect to λ_F, as follows:

$$\phi_l(z) = \sqrt{\frac{2}{L}} \sin\left(\frac{\pi l z}{L}\right) = \frac{1}{\sqrt{\lambda_F}} \sqrt{\frac{2\lambda_F}{L}} \sin\left(\frac{\pi l z/\lambda_F}{L/\lambda_F}\right)$$

$$=: \frac{1}{\sqrt{\lambda_F}} \bar{\phi}_l(z), \quad (A1)$$

with $\bar{\phi}_l(z)$ being the same for all background densities n_+, when λ_F is used as unit of length. Passing now to Eq. (12), we have

$$\gamma_{ij}(z) = \phi_i^*(z)\phi_j(z) = \frac{1}{\lambda_F} \bar{\phi}_i^*(z)\bar{\phi}_j(z) =: \frac{1}{\lambda_F} \bar{\gamma}_{ij}(z), \quad (A2)$$

and regarding the Kohn-Mattson function $g_{ij}(u)$ [23],

$$g_{ij}(u) = \frac{k_F^i k_F^j}{4\pi} \int_0^\infty \frac{d\rho}{\rho} \frac{J_1(\rho k_F^i) J_1(\rho k_F^j)}{\sqrt{\rho^2 + u^2}} =: \frac{1}{\lambda_F^3} \bar{g}_{ij}(u), \quad (A3)$$

with $\bar{g}_{ij}(u)$ being the same as $g_{ij}(u)$, but with all length scales measured in units of λ_F. Replacing everything into Eq. (11), we obtain

$$f_x^\gamma[n](z) = \frac{1}{2\pi g(z/\lambda_F)^{4/3}} \sum_{i,j}^{occ.} \int_{-\infty}^\infty d\left(\frac{z'}{\lambda_F}\right)$$

$$\times \bar{\gamma}_{ij}[(1+\gamma)z - \gamma z']$$

$$\times \bar{g}_{ij}(|z - z'|)\bar{\gamma}_{ji}[\gamma z + (1-\gamma)z'], \quad (A4)$$

which is the analytical proof of the universality of the generalized exchange enhancement factor $f_x^\gamma[n](z)$.

We note that this universality, which occurs for IBM electron densities and not, in general, for other electron-density

profiles, refers only to r_s and not to the quantum-well thickness L, as can be seen in the right lower panel of Fig. 2. On the other hand, we note that this universality also applies to the bidimensional density N/A defined just after Eq. (3) and the 2D electron-density parameter r_s^{2D} introduced just after Eq. (5), which are both kept constant in Figs. 1 and 6 as the IBM quantum well collapses from three to two dimensions. This is easily proven by noting that

$$\frac{N}{A} = a n_+ = \frac{\left(k_F^{2D}\right)^2}{2\pi} = \frac{2\pi}{\left(\lambda_F^{2D}\right)^2}, \qquad (A5)$$

with $n_+ = 8\pi/3\lambda_F^3$, so that

$$\lambda_F = \left(\frac{a}{3\pi^2 \lambda_F^{2D}}\right)^{1/3} \lambda_F^{2D}. \qquad (A6)$$

Here, a represents the width of the neutralizing jellium background.

Using Eq. (A6), it is clear that the universality displayed in Eq. (A4) with regard to r_s yields the universality of $f_x^\gamma[n](z)$ with regard to r_s^{2D} as well.

[1] P. Hohenberg and W. Kohn, Inhomogeneous electron gas, Phys. Rev. **136**, B864 (1964).

[2] W. Kohn and L. J. Sham, Self-consistent equations including exchange and correlation effects, Phys. Rev. **140**, A1133 (1965).

[3] E. Engel and R. M. Dreizler, *Density Functional Theory: An Advanced Course* (Springer, Berlin, 2011).

[4] J. P. Perdew and K. Schmidt, in *Density Functional Theory and its Applications to Materials*, edited by V. E. Van Doren, C. Van Alsenoy, and P. Geerlings (American Institute of Physics, Melville, N. Y., 2001), Vol. 577, p. 1.

[5] A. Becke, A new inhomogeneity parameter in density-functional theory, J. Chem. Phys. **109**, 2092 (1998).

[6] J. P. Perdew, S. Kurth, A. Zupan, and P. Blaha, Accurate Density Functional with Correct Formal Properties: A Step Beyond the Generalized Gradient Approximation, Phys. Rev. Lett. **82**, 2544 (1999).

[7] J. Sun, A. Ruzsinsky, and J. P. Perdew, Strongly Constrained and Appropriately Normed Semilocal Density Functional, Phys. Rev. Lett. **115**, 036402 (2015).

[8] R. M. Dreizler and E. K. U. Gross, *Density Functional Theory* (Springer-Verlag, Berlin, 1990), p. 109.

[9] C. Horowitz, C. R. Proetto, and J. M. Pitarke, Semilocal approximations to the Kohn-Sham exchange potential as applied to a metal surface, Phys. Rev. B **105**, 085149 (2022).

[10] S. Kurth, J. P. Perdew, and P. Blaha, Molecular and solid-state tests of density functional approximations, Int. J. Quantum Chem. **75**, 889 (1999).

[11] C. M. Horowitz, C. R. Proetto, and J. M. Pitarke, Towards a universal exchange enhancement factor in density functional theory, Phys. Rev. B **107**, 195120 (2023).

[12] G. Bastard, *Wave Mechanics Applied to Semiconductor Heterostructures* (Les Editions de Physique, Les Ulis, 1988).

[13] P. Harrison, *Quantum Wells, Wires and Dots* (Wiley, West Sussex, 2010).

[14] H. Rydberg, M. Dion, N. Jacobson, E. Schröder, P. Hyldgaard, S. I. Simak, D. C. Langreth, and B. I. Lundqvist, Van der Waals Density Functional Theory for Layered Structures, Phys. Rev. Lett. **91**, 126402 (2003).

[15] L. Chiodo, L. Constantin, E. Fabiano and F. Della Sala, Nonuniform Scaling Applied to Surface Energies of Transition Metals, Phys. Rev. Lett. **108**, 126402 (2012).

[16] C. M. Horowitz, S. Rigamonti, and C. R. Proetto, Kohn-Sham Exchange Potential for a Metallic Surface, Phys. Rev. Lett. **97**, 026802 (2006).

[17] C. M. Horowitz, C. R. Proetto, and J. M. Pitarke, Exact-exchange Kohn-Sham potential, surface energy, and work function of jellium slabs, Phys. Rev. B **78**, 085126 (2008).

[18] C. M. Horowitz, L. A. Constantin, C. R. Proetto, and J. M. Pitarke, Position-dependent exact-exchange energy for slabs and semi-infinite jellium, Phys. Rev. B **80**, 235101 (2009).

[19] G. F. Giuliani and G. Vignale, *Quantum Theory of the Electron Liquid* (Cambridge University Press, Cambridge, 2005).

[20] J. M. Pitarke and A. G. Eguiluz, Jellium surface energy beyond the local-density approximation: Self-consistent calculations, Phys. Rev. B **63**, 045116 (2001).

[21] L. Pollack and J. P. Perdew, Evaluating density functional performance for the quasi-two-dimensional electron gas, J. Phys.: Condens. Matter **12**, 1239 (2000).

[22] A. D. Kaplan, K. Wagle, and J. P. Perdew, Collapse of the electron gas from three to two dimensions in Kohn-Sham density functional theory, Phys. Rev. B **98**, 085147 (2018).

[23] W. Kohn and A. E. Mattsson, Edge Electron Gas, Phys. Rev. Lett. **81**, 3487 (1998).

[24] J. P. Perdew, A. Ruzsinszky, J. Sun, and K. Burke, Gedanken densities and exact constraints in density functional theory, J. Chem. Phys. **140**, 18A533 (2014).

[25] There is a difference here with the self-consistent slab model of our previous work, for which the bounded behavior was obtained for $0.25 \leqslant \gamma < 0.75$. This is due to the fact that the asymptotic behavior of the electronic density is different in these models.

[26] The GGA's and meta-GGA's exchange enhancement factors $F_x(s)$ and $F_x(s, \alpha)$, respectively, are known not to depend on the local electron density, thus satisfying the constraint $E_x[n_\lambda] = \lambda E_x[n]$ under uniform scaling, i.e., with $n_\lambda(\mathbf{r}) = \lambda^3 n(\lambda \mathbf{r})$ [35].

[27] M. Lewin, E. H. Lieb, and R. Seiringer, Improved Lieb-Oxford bound on the indirect and exchange energies, Lett. Math. Phys. **112**, 92 (2022).

[28] J. Perdew and J. Sun, The Lieb-Oxford Lower Bounds on the Coulomb Energy, their importance to electron density functional theory, and a conjectured tight bound on exchange, in *The Physics and Mathematics of Elliott Lieb. The 90th Anniversary Volume II*, edited by R. L. Frank, A. Laptev, M. Lewin, and R. Seiringer (EMS Press, 2022), ch. 36, pp. 165–178.

[29] E. Räsänen, S. Pittalis, K. Capelle, and C. R. Proetto, Lower Bounds on the Exchange-Correlation Energy in Reduced Dimensions, Phys. Rev. Lett. **102**, 206406 (2009).

[30] T. Aschebrock and S. Kümmel, Ultranonlocality and accurate band gaps from a meta-generalized gradient approximation, Phys. Rev. Res. **1**, 033082 (2019).

[31] L. A. Constantin, Dimensional crossover of the exchange-correlation energy at the semilocal level, Phys. Rev. B **78**, 155106 (2008).

[32] J. P. Perdew, K. Burke, and M. Ernzerhof, Generalized Gradient Approximation Made Simple, Phys. Rev. Lett. **77**, 3865 (1996).

[33] J. Sun, B. Xiao, and A. Ruzsinszky, Effect of the orbital-overlap dependence in the meta generalized gradient approximation, J. Chem. Phys. **137**, 051101 (2012).

[34] J. Sun, R. Haunschild, B. Xiao, I. W. Bulik, G. E. Scuseria, and J. P. Perdew, Semilocal and hybrid meta-generalized gradient approximations based on the understanding of the kinetic-energy-density dependence, J. Chem. Phys. **138**, 044113 (2013).

[35] M. Levy and J. P. Perdew, Hellmann-Feynman, virial, and scaling requisites for the exact universal density functionals. Shape of the correlation potential and diamagnetic susceptibility for atoms, Phys. Rev. A **32**, 2010 (1985).